임펄스 잡음에 의해 훼손된 이진 디지탈 서류 영상의 복구 방법들의 비교 평가

신 현 경[†] · 신 중 상[††]

요 약

디지탈 변환과 기기간의 전송 영향으로 화질이 떨어진 디지탈 영상의 복구는 잡음 발생 및 그 역 과정의 모형화를 통해 이루어낼 수 있다. 스캐너로 읽혀진 서류 영상이나 위성 사진에서 잡음 및 반점을 제거하는 과정이 좋은 예이다. 그러나 잡음 발생의 비선형성은 그 역 과정의 이론적 이해를 어렵게한다. 본 논문에서는 충격 잡음에의해 화질이 떨어진 이진 서류 영상의 복구 방법들을 심층 분석하는 것에 촛점을 맞추었다.

본 연구 결과에 의하면 이진 서류 영상의 잡음 제거 방식으로 '가중 중앙값' 여과기와 '리' 여과기가 다른 여과기에 비해 효과적임을 보여준다. 반면 '웨이브렛' 여과 방식은 타 방식보다100여배의 시간이 소요되어 비 효율적이다. 본 논문에서는 가중 중앙값 여과기에 쓰이는 가중치에 대한 연구 결과를 제시하였다.

키워드 : 영상 처리, 서류 영상, 영상 복구, 영상 정화, 잡음 제거 여과

Evaluation of Restoration Schemes for Bi-Level Digital Image Degraded by Impulse Noise

Hyun-Kyung Shin[†] · Joong-Sang Shin[††]

ABSTRACT

The degradation and its inverse modeling can achieve restoration of corrupted image, caused by scaled digitization and electronic transmission. De-speckle process on the noisy document(or SAR) images is one of the basic examples. Non-linearity of the speckle noise model may hinder the inverse process. In this paper, our study is focused on investigation of the restoration methods for bi-level document image degraded by the impulse noise model.

Our study shows that, on bi-level document images, the weighted-median filter and the Lee filter methods are very effective among other spatial filtering methods, but wavelet filter method is ineffective in aspect of processing speed: approximately 100 times slower. Optimal values of the weight to be used in the weighted median filter are investigated and presented in this paper.

Key Words : Image Processing, Document Imaging, Image Restoration, Image Clean-Up, And De-Speckle Filters

1. Introduction

Burst of coherent radiation of active radar sensor, corrupted electronic transmission used in fax and scanner, or digitization scaling engenders the specks and noises appeared in digital images. For a computer generated document image, existence of noises in electronic image is the cause of at least two bad consequences: first of all, it increases the size of document file resulting in wasting of disk storage(about 120% to 600% reduced space depending on the residence of noises) and secondly, it worsens performance in both time and quality of optical object recognition processes such as barcode recognition, O.M.R., O.C.R., and I.C.R., which take the chief roles in document imaging industry.

The key subject on restoration from corrupted digitization is in comprehension of degradation procedure which can be modeled as degradation function, $h(x, y)$, and additive noise, $\iota(x, y)$ is. The mathematical formulation of degradation process can be described as follows[1]:

$$g(x, y) = h(x, y) * f(x, y) + \iota(x, y), \quad (1)$$

where f(x, y) represents the input image. Unlike other important

† 정 회 원 : 경원대학교 수학정보학과 강사
†† 정 회 원 : 경원대학교 수학정보학과 교수
논문접수 : 2006년 3월 22일, 심사완료 : 2006년 6월 2일

imaging formats adapted by remote sensing SAR(synthetic aperture radar) images, medical images(DICOM) or digital photo images, having 8 to 64 bit scale for their pixel representation, a document image without picture included can be represented by binary pixel value. ISO/IEC standards CCITT-3[2]/CCITT-4 [3] and JBIG[4]/JBIG2[5] were proposed in order for scanned or faxed bi-level document images to save their file sizes[6]. Having its pixel value in one bit, i.e., the range of pixel value is {0, 1}, bi-level images lead most of noise models such as Gaussian, Raleigh, Gamma, and Exponential to be ineffective for study of bi-level image restoration. Only suitable noise model is the 'saturated salt and pepper style impulse noise'. Due to binary property of its pixel value, in document imaging, degradation function described at (1) h(x, y) is usually considered as identity transformation, i.e., noise only degradation. In this type of situation, frequency domain methods adapting noise filtering techniques by detection of abnormal frequencies is not effectual than spatial filtering methods.

Various de-speckling and de-noising techniques have been offered as depicted below. As stated in[1], some restoration techniques are formulated in the spatial domain while the others are formulated in the frequency domain. The simple spatial morphological filters such as mean filter[1] and median filter[7] have evolved to the advanced forms in which local statistics of pixel neighborhood is of great concerns: Lee[8], Lee-Sigma[9], Frost[10], Gamma-MAP[11, 12], Kuan[13], local region[14], and modified (weighted) median[1]. Each method will be explained later in this paper. On the other hand, the frequency filters usually based on the wavelet transformation also have been developed[15-20]. [15, 16] are the research framework for wavelet based de-noising methods. The wavelet-based speckle removal methods are proposed on medical images[17], and on SAR images[18-20]. Besides the spatial-and frequency domain methods, with application of elliptic PDE, a new approach called non-isotropic diffusion, typically accepted in image segmentation, has been introduced[21]. Comparative studies between various de-noising filters for SAR images are presented[22-24].

The aim of this paper is to rigorously evaluate the noise filtering methods to find properly representing restoration process of the impulse noise model applied in binary document image. Since no multiplicative noise is assumed in binary image, as mentioned above, spatial domain filtering is more convincing than frequency domain filtering. For the comparability of test, we tested both spatial and frequency-domain filter methods: Frost, Gamma-MAP, local region, Lee, Lee-Sigma, modified median and classic Daubechies' wavelet filter[12, 13].

Organization of this paper is as follows. In §2, each filter method exploited in this paper is briefly explained. In §3, test data and specification of system on which tests were performed is described. In §4, test results and discussion are presented.

2. Restoration Methods

In this section the de-speckle methods employed in this paper are introduced briefly.

Frost filter uses a minimum mean square error algorithm which, adaptive filtering exponentially damped convolution kernel, adapts to the local statistics of the image to preserve edges and small features. The formula with convolution kernel is

$$D = \sum_{n\times n} A\ a\ k(a,t)$$
$$\text{where } a = (4/n\rho^2)(\sigma^2/m^2) \qquad (2)$$
$$k(a,t) = e^{-a|t|}$$

where a is the local coefficient of variation, A is the normalization constant, ρ is the image coefficient of variation, σ is the local variance, m is the local mean, and t denotes the distance from the pixel of interest. The resulting digital number D will replace the pixel value.

MAP(Maximum A-Posteriori) filter maximizes the a posteriori probability density function. This filter assumes that the original pixel value lies between that of the pixel of interest and the moving window average. This algorithm incorporates the assumption that the noise has Gamma distribution based on a multiplicative noise model with non-stationary mean and variance parameters. An analytic solution[25] of the following cubic equation,

$$x^3 - m \cdot x^2 + \sigma \cdot (x - v) = 0 \qquad (3)$$

where v, m and σ are given pixel value, local mean and local variance, respectively, will replace the pixel value.

Local region filter divides the moving window into eight rectangular regions based on angular position. Once variance is calculated locally for each region, the pixel of interest is replaced by the mean of all pixel values within the region with the lowest variance.

$$\sigma_{\text{Imin}} = \min \{ \sigma_1, \sigma_2, \sigma_3, \sigma_4, \sigma_5, \sigma_6, \sigma_7, \sigma_8 \} \qquad (4)$$

where σ_i denotes local variance in the specified i-th region.

$$D = \langle p \rangle \text{ for all } p \in I_{min} \text{ region} \qquad (5)$$

where the bracket indicates averaging. The digital number D is the candidate replacing the pixel value.

In practice, it can be used sequentially two or three times, increasing the window size with each pass.

Based on the assumption that the mean and variance of the pixel of interest is equal to the local mean and variance of all pixels within the user-selected moving window, Lee-Sigma filter utilizes the statistical distribution of the pixel values within the moving rectangular window. For a given window, the sigma value is computed as

$$\Sigma = \sqrt{(\sigma^2/m^2)} \qquad (6)$$

where σ^2, m are local variance and mean, respectively.

It uses the average of all pixel values within the moving window that fall within the designated range of standard deviation.

$$D = \langle \{ p \mid (1 - w\Sigma)p_0 < p < (1 + w\Sigma)p_0 \} \rangle \qquad (7)$$

where p_0 is the given pixel value, Σ is global variance as seen in Eq. (6), and $w = 2$ in this paper.

In practice, Lee-Sigma filter and local region filter can be a successive pass iteratively for better resultant image.

One of the most widely used noise reduction filter in camera industry, the Lee filter is able to smooth away noise in flat regions, but leave fine details(such as lines and text) unchanged. Like the Lee Sigma filter, Lee filter is based on assumption that the mean and the variance of the pixel of interest is equal to the local mean and variance of all pixels in the specific moving windows. Within each window, the local mean and variance are estimated. In regions of no signal activity, the filter outputs the local mean. Its major drawback is that it leaves noise in the vicinity of edges and lines.

A well-known nonlinear method is the median filter that, useful for removing impulse(salt and pepper, pulse or spike) noises[1], finds the median value in a given window to replace the value of the pixel of interest. A main drawback of this method is blurring/eroding effect at the black and white pixel boundary. Switching scheme (performs filtering at only the pixels of interest, for example only at black pixels) is an alternative method to resolve this problem. In addition, the modified(weighted) median filtering shows more effectiveness. This weighted median filter replaces a pixel value of interest with a specified percentile(70%, for example) rather than median. In section 4 we present the optimal value for percentile.

〈Table 1〉 Dimension of Test Images

Noise Type	Size	Resolution	File Size	Colors	Noise
High Level	1728 × 2144 in pixel	204 × 196 DPI	454 Kb	2	10%
Low Level	1728 × 2144 in pixel	204 × 196 DPI	454 Kb	2	7%
Correlated	1728 × 2144 in pixel	204 × 196 DPI	454 Kb	2	8.8%

3. Test Data and Computer System Specification

Generation of Noises: For the study of this paper, we generated three types of impulse noises: high level, low level, and vertically correlated. In order for producing high and low level noises in each white pixel, Gaussian noise is generated and then compared with the given threshold. The higher threshold produces the higher level noises. In this paper, the image with higher level noise has 10% noise level which means that 10% of white pixels switched to noise. The image with lower level noise has 7% noise level. The vertically correlated noises were created by low quality scanner and printer. We printed and scanned the original image to get the noisy image.

Image Acquisition: The sample images in presence of noise, as seen in Figure 1, were obtained from commercial .NET SDK software DotImageTM of Atalasoft, Inc. The original test image is an e-faxed document saved in TIFF as CCITT Group4 format. We added low-level and high-level noises(See A.1, B.1 in Figure 1) using random generator as explained in the previous paragraph, and correlated noise(See C.1 in Figure 1). The dimensions of test images are as follows:

Computer Programming Language : For the de-noising filters described in this paper, Microsoft Visual C# in .Net Framework was used to write programming code.

Computer System Specification : In this paper tests were performed on PC with AMD AthlonTM XP 1800+ 1.5 GHz and 512 MB of RAM.

4. Experimental Results and Discussion

Our study is focused on comparison among filtering methods. Before presenting our results, it is required to mention compatibility of the sample images and filters. We have performed experiments with various types of images: different resolutions, noise levels, impulse noise model with diverse underlying random generators(Gaussian, Raleigh, and Exponential). At first, resolution issue is important since boundary between speck and noise can be affected. Image filtering is a discrete version of function convolution. To verify that filtering process is independent on image resolution,

the scale invariance property of convolution operation is described. For convenience of understanding, notations for functional symbol are tabulated as follows: I^{cR}_S, I^{cR}_P, I^{fR}_S, I^{fR}_P, where superscripts cR and fR indicate coarse and fine resolution, respectively, and subscripts s and p signify source and processed images, respectively. Suppose that two images, I^{cR}_S and I^{fR}_S, are acquired from the same source with different resolution. Then the following consequence of relations can be derived between the two images:

$$I^{cR}_S(x, y) = I^{fR}_S(ax, by), \text{ where } a > 1, b > 1,$$
$$I^{cR}_P(x, y) = \langle I^{cR}_S * g \rangle(x, y)$$
$$= \langle I^{fR}_S * g \rangle(ax, by) = I^{fR}_P(ax, by),$$
$$\text{i.e., } I^{cR}_P(x, y) = I^{fR}_P(ax, by),$$

where the convolution operation $\langle I * g(x, y) \rangle = \int\int I(s, t) \cdot g(s-x, t-y)\, ds\, dt$.

Secondly, our presumption "there is no dependence between noise level(of impulse noise with underlying Gaussian random generator) and performance because of the local property of filter masking method" is confirmed by the experiment. We present high and low level noise models to confirm this. However, processing time was reduced in low level noise, which was caused by the switching scheme(skipping white pixels). So we can still affirm that noise level doesn't affect performance of noise reduction by filtering. Refer to <Table 2> Finally, in binary image, conventional underlying random generators(Raleigh, Gauss, Exponential) used to produce impulse noise didn't affect filtering performance. Refer to <Table 2>.

To provide evidence the statements above that performance of filtering process is independent on the underlying random generators and the image noise level, we present the statistical analysis data on a relative error, η, and noise removal rates, ϕ, in the <Table 2>. The simulations are performed by a 3×3 median filter with pure noise images created by three different noise model, Gaussian, Exponential, and Raleigh generator. Each random generator constructs 5 images with different noise levels, 0.01, 0.03, 0.05, 0.10, and 0.15. Proximity of each row gives an evidence of random generator independence, and that of each column demonstrates noise level independence.

From now on, performance comparison between filters will be discussed. The three types of noise model are exercised: high level, low level, and machine inducing vertically correlated noise. Please refer to section 3 for detailed description of noise types. Six of conventional filtering method plus wavelet method are evaluated. The sample images in presence of noise and the restored images are become visible in (Figure 1) at the left side of the table are the images in the presence of noise and at the right

〈Table 2〉 Independence of noise level and underlying random generator on filtering performance.

		Random Generator					
		Gaussian		Raleigh		Exponential	
		η	ϕ	η	ϕ	η	ϕ
approximate noise level	0.01	0	1	0	1	0	1
	0.03	0	1	0	1	0	1
	0.05	0.0017	0.9994	0.0014	0.9994	0.0014	0.9997
	0.10	0.0142	0.9921	0.0114	0.9936	0.0142	0.9921
	0.15	0.0487	0.9720	0.0430	0.9746	0.0448	0.9741

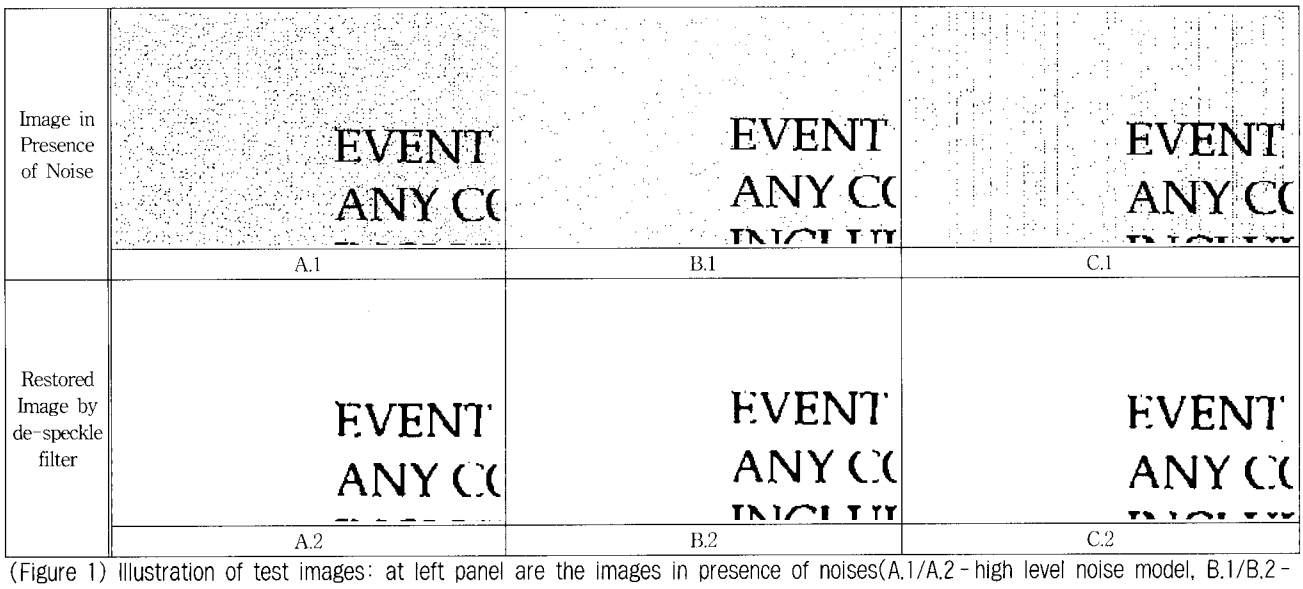

(Figure 1) Illustration of test images: at left panel are the images in presence of noises(A.1/A.2 - high level noise model, B.1/B.2 - low noise model, C.1/C.2 - correlative noise model) and at right panel are the images with noises removed by restoration process.

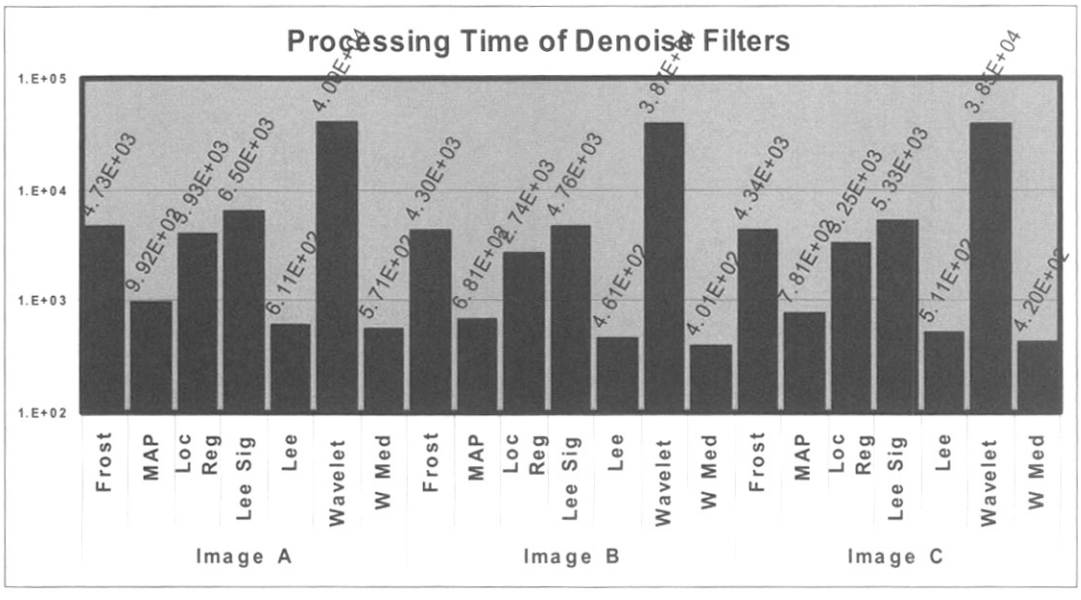

(Figure 2) Processing time in millisecond(1/1000sec). The acronyms "Loc Reg", "Lee-Sig", and W-Med" denote "Local Region", "Lee-Sigma", and "Weighted Median", respectively. Image A, B, and C stand for the images representing high, low level, and correlated noises, respectively.

〈Table 3〉 Reduction of file size is presented. "Noised" and "Restored" represent the image in presence of noises and the image after de-noising process, respectively. The unit of file size is Kilo-Byte.

Image	File Saving Methods	High Level Noise	Low Level Noise	Correlated Noise
Noised	CCITT-G4 TIFF	271	78	145
	JPEG	1,896	908	1,250
Restored	CCITT-G4 TIFF	43	41	36
	JPEG	539	539	540

side are the images after reduction of noises by the filters. The images illustrated in the table were cropped, size of 200×75 in pixel with fixed ranged of coordinates[(100, 100), (300, 175)], to preserve shape of the noises and speckles(Automatic resizing operation at some stage in inserting our image in Word diminishes noises or converts them to gray scale). For simplicity of presentation, we present only the results from the Lee filter.

Reduction of file size on behalf of de-noising/de-speckling process can be observed in <Table 3>: the file size of restored image is reduced by 47% - 85% compared to that of image with noise. We can also notice that CCITT G-4 is better format than JPEG for saving 1 bit bi-level image into file. For the JPEG compression, we used typical 75% quality level from the range of 0 to 100.

The main topic of our study between de-noise filters is in comparison of "processing time", "relative error levels", and "noise removal rates". At first, we evaluate the processing time for each method. The result is seen in (Figure 2). As the figure shows, the weighted median, the γ_0-MAP and the Lee filters are the fastest. The wavelet filter is the slowest, which is anticipated because of its frequency domain transformation. For the other filtering methods such as the Frost filter, the local region filter, and the Lee-Sigma filter have bottle neck of heavy computation. For the Frost, computation of the kernel function, for the local region filter, estimation of the eight different local variances in each pixel, for the Lee-Sigma filter, evaluation of local variance in each pixel costs a lot of operations to slow down the whole process.

Secondly, the relative error level of restoration η is estimated as below:

$$\eta = |R - O| \;/\; |D - O|, \qquad (8)$$
$$\text{where} |R - O| / |D - O| = \sum\sqrt{(r_{ij} - o_{ij})^2} \;/\; \sum\sqrt{(d_{ij} - o_{ij})^2}$$

where $\boldsymbol{R}$, $\boldsymbol{O}$, and $\boldsymbol{D}$ denote the restored image, the original image without presence of noise, and the degraded image by noise, respectively. As described in the second line of Eq. (8), the absolute value is evaluated by mean square of pixel-by-pixel distance. Ideally, if the restored image is same with the original image, η is zero. $\eta = 1$ implies no restoration. In general, the bigger value of η indicates the poorer restoration result. As seen in Figure 3, the local region filter shows excellent performance while it has problem with processing time as seen previously. The Frost, the γ MAP, the Lee, and the weighted median filters are also good. On the other hand, a drawback of the Lee-sigma filter, inability of removing noises at the character boundary, is revealed.

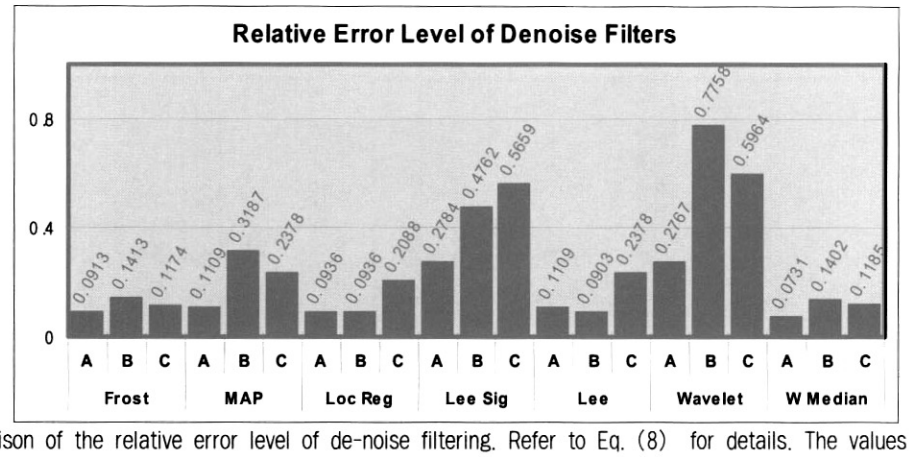

(Figure 3) Comparison of the relative error level of de-noise filtering. Refer to Eq. (8) for details. The values are dimensionless. The acronyms "Loc Reg", "Lee-Sig", and W-Med" denote "Local Region", "Lee-Sigma", and "Weighted Median", respectively. A, B, and C stand for the images in Figure 1 representing high, low level, and correlated noises, respectively.

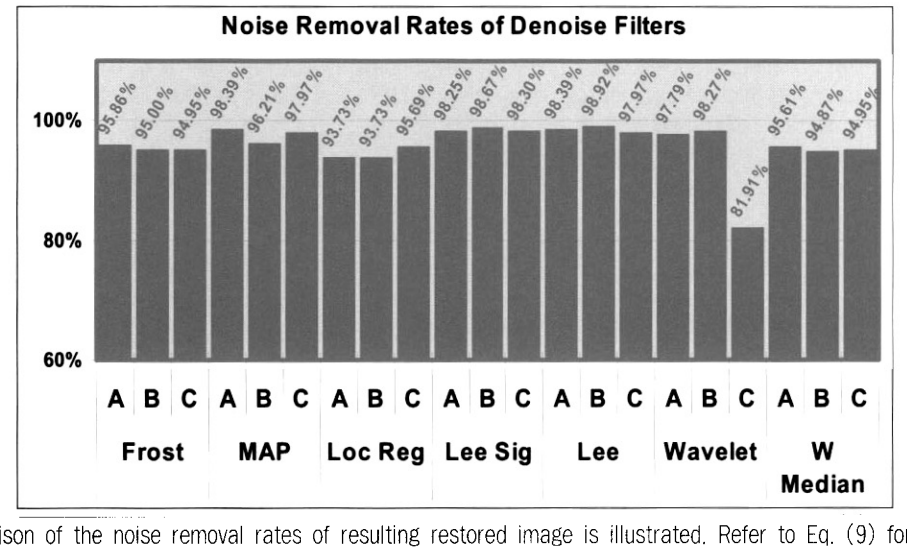

(Figure 4) Comparison of the noise removal rates of resulting restored image is illustrated. Refer to Eq. (9) for details. The values are dimensionless. The acronyms "Loc Reg", "Lee-Sig", and W-Med" denote "Local Region", "Lee-Sigma", and "Weighted Median", respectively. A, B, and C indicate the test images defined in the (Figure 1)

The relative error levels introduced above offered a method of rigorous mathematical quantification of restoration performance. It indicates an error level on identifying noises of the given filter. Now, we introduce a new indication of performance quality, the noise removal rates, ϕ. This concentrates on the rates of removal pure noises while excluding the case when a filter identifies a pixel in character as noise. This is a practical measurement especially when we use the switching scheme(skipping either black or white pixels).

Thirdly, the noise removal rates ϕ are calculated as follows:

$$\phi = |R - D|_b \;/\; |O - D| \qquad (9)$$

$$\text{where } |R - D|_b \;/\; |D - O| = \Sigma \max(r_{ij} - d_{ij},\ 0) \;/\; \Sigma \sqrt{(d_{ij} - o_{ij})^2}$$

R, D, and O are used as the same manner in Eq. (8). $|R - D|$ and $|D - O|$ are the number of removed pixels and the total number of degraded pixels, respectively. Since we already have the original image without noise, obtainment of values of $|R - D|$ and $|D - O|$ is straightforward from direct pixel-by-pixel comparison among original, degraded, and restored images. In Eq. (9), in case the resulting ϕ = 1 means perfect removal of noises, while ϕ = 0 does no removal of noises. As seen in (Figure 4), the Lee and the Lee-Sigma show excellent performance, the γ-MAP, the Frost, and the weighted median show good performance.

Finally, in this paper, we present our interesting discovery on the optimal values for the weighted median filter. The value for weight(of a weighted median filter) affect on the restoration process in serious manner. For a reminder, the conventional median filter is a weighted median with 50 percentile. For examples, in 3 by 3 windows 5-th value out of 9 data(after sorting) will replace the pixel value; in

〈Table 5〉 Finding of optimal weight value: η and φ are defined in Eqs. (8), (9), respectively. The second column indicates the modified median value and its corresponding percentile. Figure 1, A.1, B.1, and C.1 stand for the images in the table representing high, low level, and correlated noises, respectively.

		Figure 1 A.1		Figure 1 B.1		Figure 1 C.1	
Filter size	Order(%)	η	φ	η	φ	η	φ
3×3	4/9(44)	0.1109	0.9039	0.9038	0.9892	0.2378	0.8449
	5/9(55)	0.0731	0.9561	0.3187	0.9622	0.1186	0.9795
	6/9(66)	0.0998	0.9884	0.1402	0.9488	0.1763	0.9797
	7/9(77)	0.3427	0.6573	0.1017	0.8989	0.4547	0.5454
5×5	13/25(52)	0.3163	0.9791	0.4501	0.9859	0.7183	0.9806
	14/25(56)	0.2288	0.9666	0.4054	0.9707	0.5166	0.9701
	15/25(60)	0.1580	0.9582	0.2963	0.9631	0.3197	0.9622
	16/25(64)	0.1257	0.9499	0.1816	0.9552	0.2293	0.9524
	17/25(68)	0.1082	0.9403	0.1568	0.9483	0.1810	0.9398
	18/25(72)	0.1002	0.9275	0.1398	0.9394	0.1594	0.9181
	19/25(76)	0.1012	0.9116	0.1240	0.9214	0.1533	0.8832

5 by 5 windows 13-th value out of 25 data(after sorting) will do the job. It is well known fact that the conventional median filter has problem with eroding foreground/background boundaries due to the boundary geometry of the foreground. To avoid the erosion, weighted median is frequently applied[1, 26].

In <Table 5>, we present relative error levels and noise removal rates from modified median filter method. At the first column are filtering window sizes indicated, and at the second column are the modified median and its corresponding percentile shown. As seen in the table, 55 - 66 percentile(when 3×3 windows are used), and 60 - 72 percentile(when 5×5 windows are used) are good candidate for the optimal value of weight.

References

[1] Gonzalez, R. C. and Woods, R. E., "Digital Image Processing," 2nd Edition, Prentice-Hall, 2002.

[2] CCITT Recommendation T. 4, "Standardization of Group 3 Facsimile Apparatus for Document Transmission," 1981.

[3] CCITT Recommendation T. 6, "Facsimile Coding Schemes and Coding Control Functions for Group 4 Facsimile Apparatus," 1986.

[4] ITU-T Recommendation T.82|ISO/IEC 11544:1993, "Coded representation of Picture and Audio Information -Progressive Bi-Level Image Compression," 1992.

[5] ITU-T SG8|ISO/IEC JTC 1/SC 29/WG1 14493:1999, "Information Technology - Coded Representation of Pictures and Audio Information - Lossy/lossless Coding of Bi-level Images," 1999.

[6] Urban, Stephen J., "Review of Standards for Electronic Imaging for Facsimile systems," Journal of Electronic Imaging, Vol.1, No. 1, pp.5 - 21, Jan, 1992.

[7] Intel, "Fast Algorithms Median Filtering," A79835-2001, 2001.

[8] Lee, J. S., "Digital Image Enhancement and Noise Filtering by Use of Local Statistics," IEEE Trans. on PAMI, Vol.2, No.2, pp.165-168, 1980.

[9] Lee, J. S., "Refined Filtering of Image Noise Using Local Statistics," CGIP, Vol.15, pp.380-389, 1981.

[10] Frost, V., Stiles, J., Shanmugan, K., and Holtzman, J., "A Model for Radar Images and Its Application to Adaptive Digital Filtering and Multiplicative Noise," IEEE Trans. on PAMI, Vol.4, pp.157-166, Mar., 1982.

[11] Lopes, A., Nezry, E., Touzi, R., and Laur, H., "Structure Detection and Statistical Adaptive Speckle Filtering in SAR Image," Int. J. Remote Sensing, Vol.14, pp.1745-1758, June, 1993.

[12] Donoho, D. L., "De-noising by soft-thresholding," IEEE Trans. On Inf. Theory, Vol.41, No.3, 1995.

[13] Kuan, D. T., Sawchuk, A. A., Strand, T. C., Chavel, P., "Adaptive noise smoothing filter for images with signal dependent noise," IEEE Trans. on Pattern Analysis and Machine Intelligence, Vol.7, No.2, pp.165-177, 1985.

[14] Rangayyan, R. M., Das, A., "Filtering multiplicative noise in images using region-based statistics," Journal of Electronic Imaging, Vol.7, No.1, pp.222-230, Jan., 1998.

[15] Daubechies, I., "Orthonormal Bases of Compactly Supported Wavelets," C.P.A.M., Vol.41, No.7, pp.909-996, 1988.

[16] Laine, A. F. and Zong, X., "A Multiscale Sub-Octave Wavelet Transform for De-Noising and Enhancement," Wavelet Applications in Signal and Image Processing IV, Proceedings of SPI, Vol.2825, pp.238-249, Denver, CO, 1996.

[17] Achim, A., Bezerianos, A., and Tsakalides, P., "Novel Baysian multiscale methods for speckle removal in medical

ultrasound images," IEEE Trans. Med. Imaging., Vol.20, pp.772-783, Aug., 2001.

[18] Achim, A., Tsakalides, P., Bezerianos, A., "SAR Image Denoising via Baysian Wavelet Shrinkage Based on Heavy-Tailed Modeling," IEEE Trans. on Geosci. and Remote Sensing, Vol.41, No.8, Aug., 2003.

[19] Xie, H., Pierce, L. E., and Ulaby, F. T., "SAR speckle reduction using wavelet denoising and Markov random field modeling," IEEE Trans. on Geosci. and Remote Sensing, Vol.40, pp.2196-2212, Oct., 2002.

[20] Xie, H., Pierce, L. E., and Ulaby, F. T., "Statistical properties of logarithmically transformed speckle," IEEE Trans. on Geosci. and Remote Sensing, Vol.40, pp.721-727, Mar., 2002.

[21] Yu, Y., Acton, S. T., "Speckle Reducing Anisotropic Diffusion," IEEE Trans. on Image Processing, Vol.11, No.11, Nov., 2002.

[22] Lee, J. S., Jurkevich, I., Dewaele, P., Wambacq, P., Oosterlinck, A., "Speckle filtering of synthetic aperture radar images: a review," Remote Sensing Review, Vol.8, pp.313-340, 1994.

[23] Gagnon, L, and Jouan, A., "Speckle filtering of SAR images - a comparative study between complex-wavelet based and standard filters," SPIE proc. No.3169, pp.89-91, 1997.

[24] Desnos, Y. L., and Matteini, V., "Review on structure detection and speckle filtering on ERS-1 images," EARSel Advances in Remote Sensing, Vol.2, No.2, pp.52-65, 1993.

[25] Uspensky, R.V., "Theory of Equations," New York, McGraw-Hill, 1948.

[26] Jain, A. K. "Fundamentals of Digital Image Processing," Prentice-Hall, 1990.

신 현 경

e-mail : hyunkyung@kyungwon.ac.kr

2002년 S.U.N.Y. Stony Brook 응용수학과(공학박사)

2002년~현재 경원대학교 수학정보학과 강사

관심분야 : image processing and analysis, artificial neural network, computational geometry, scientific computing, optical character recognition and computational vision.

신 중 상

e-mail : jsshin@kyungwon.ac.kr

1969년 서울대학교 사범대학(학사)

1982년 서강대학교(이학석사)

1987년 서강대학교(이학박사)

1982년 인천교대학교 수학교육학과 조교수

1988년~현재 경원대학교 수학정보학과 교수

관심분야 : image algebra, operation research, artificial neural network, financial mathematics.